The Japanese Geotechnical Society

SOILS AND FOUNDATIONS Vol. 24, No. 4, 30-48, Dec. 1984
Japanese Society of Soil Mechanics and Foundation Engineering

STRENGTH AND DEFORMATION CHARACTERISTICS OF SATURATED SAND AT EXTREMELY LOW PRESSURES

Shinji Fukushima* and Fumio Tatsuoka**

ABSTRACT

A series of drained triaxial compression tests at extremely low pressures was performed on saturated samples of fine, angular sand to know the dependency of both the angle of internal friction $\phi = \arcsin\{(\sigma_1' - \sigma_3')/(\sigma_1' + \sigma_3')\}_{max}$ and the deformation characteristics on the value of σ_3'. Great cares were paid to the stress measurements and the stress corrections for membrane forces. Also in order to confirm the results with respect to the value of φ, several analyses based both on the stress-dilatancy relations at failure and on the deformation characteristics of sample were performed. It was found that the change of ϕ with the change of σ_3' is very small when σ_3' is lower than around 0.5 kgf/cm^2 (50 kN/m^2), especially lower than around 0.1 kgf/cm^2 (10 kN/m^2). It was also found that the apparent cohesion intercept is not needed in using the Mohr-Coulomb failure criterion for the saturated sand tested. Further, it was found that the change of deformation characteristics of sand with the change of σ_3' is rather small when σ_3' is lower than around 0.5 kgf/cm^2 as well.

Key words: angle of internal friction, dilatancy, drained shear, sandy soil, shear strength, triaxial compression test (**IGC**: D 6)

INTRODUCTION

The values of the angle of internal friction defined as $\phi = \arcsin\{(\sigma_1' - \sigma_3')/(\sigma_1' + \sigma_3')\}_{max}$ of cohesionless soils at low stresses are needed for the analyses of for instances shallow failures of sand slopes and for the determination of stress-strain relations at extremely low effective stresses during cyclic undrained tests on saturated sand specimens. These are also needed to analyze the results of model tests using sand boxes such as bearing capacity tests, earth pressure tests or the like. However, only a very limited number of the values of ϕ at low stresses lower than, say, 0.5 kgf/cm^2(50 kN/m^2) have been reported in literature (Ponce and Bell, 1971, Stroud, 1971). Figs. 1(a) and (b)

* Research Engineer, Fujita Technical Laboratory, Fujita Corp., 74 O-dana-cho, Kohoku-ku, Yokohama, Kanagawa. Formerly, Graduate Student of University of Tokyo.
** Associate Professor, Institute of Industrial Science, University of Tokyo, 22-1 Roppongi 7, Minato-ku, Tokyo 106.
Manuscript was received for review on January 6, 1984.
Written discussions on this paper should be submitted before July 1, 1985, to the Japanese Society of Soil Mechanics and Foundation Engineering, Sugayama Bldg. 4F, Kanda Awaji-cho 2-23, Chiyoda-ku, Tokyo 101, Japan. Upon request the closing date may be extended one month.

NII-Electronic Library Service

The Japanese Geotechnical Society

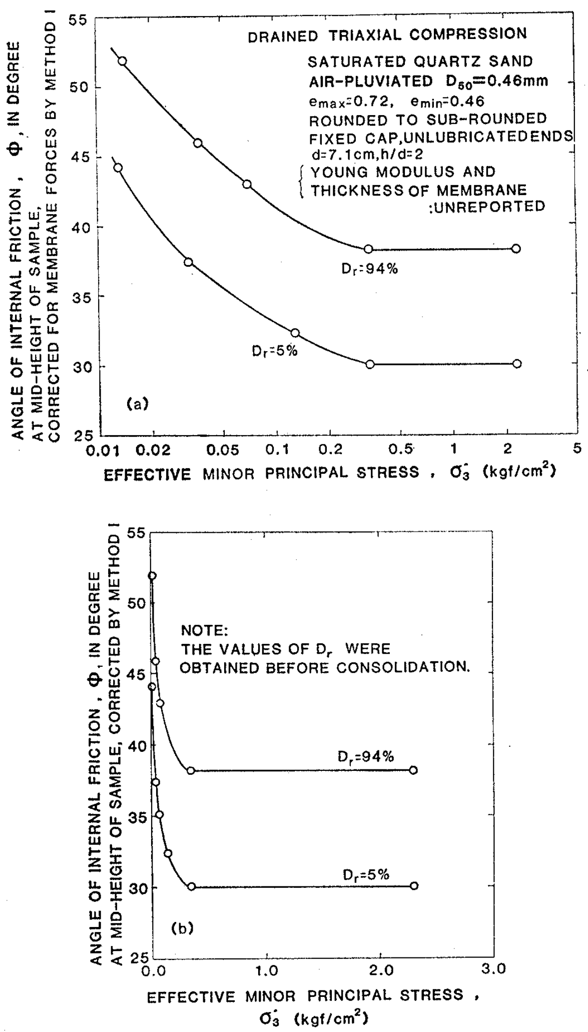

Fig. 1. Change of angle of internal friction by the change of effective minor principal stress in triaxial compression test (reproduced from Ponce and Bell, 1971) (1kgf/cm^2=98kN/m^2)

were reproduced from Ponce and Bell (1971), in which the value of ϕ has been plotted against the minor principal stress σ_3' (a) in the logarithmic scale and (b) in the arithmetic scale. The membrane forces have been corrected for these data by Method I which will be described in detail in the latter part. These values of ϕ were obtained by the conventional drained triaxial compression tests. It may be seen from these figures that the value of ϕ increases very sharply with the decrease in σ_3' when σ_3' is lower than around 0.2 kgf/cm^2 (20 kN/m^2). These results suggest that if these results are true there is some amount of the apparent cohesion intersept for this sand. However, it is also true that if the value of ϕ changes so largely with the change of σ_3' at low stresses as shown in Fig. 1, it becomes very complicated and also very difficult to analyze the results of model tests performed on small model sand grounds. Also, in such a case, the angle of internal friction at extremely low pressures should be evaluated for each different kind of sand used for model tests, because the manner of the change of ϕ with the change of σ_3' at low stresses might be very different among different kinds of sand.

In view of the above, the authors performed a series of drained triaxial compression tests for a wide range of confining pressure from 0.02 kgf/cm^2 (2.0 kN/m^2) to 4 kgf/cm^2 (392 kN/m^2) on Toyoura sand which has been used extensively in model tests at the Institute of Industrial Science, the University of Tokyo (Fukushima, 1982). In this paper it will be shown that the dependency of the value of ϕ of Toyoura sand, which is fine, angular sand, on σ_3' at low stresses is much smaller than that shown in Fig. 1 and the value of ϕ is almost independent of σ_3' when σ_3' is lower than around 0.1 kgf/cm^2 (10 kN/m^2). In addition to this, it will also be shown that to obtain an adequate conclusion with respect to this problem, great cares should be paid to the stress measurements and also the membrane forces should be properly accounted for Furthermore, it will be presented that the deformation characteristics of the sand do not change so much with the change in σ_3' when σ_3' is lower than around 0.5 kgf/cm^2 (50 kN/m^2), especially lower than around 0.1 kgf/cm^2 (10kN/m^2).

TEST PROCEDURE

In this testing program (Table 1), Toyoura sand, uniform sand, having a mean grain size of 0.16 mm, a uniform coefficient of 1.46, a specific gravity G_s=2.64 and an angular shape was used. The maximum

NII-Electronic Library Service

Table 1. List of tests

(1) Test No.	(2) σ_c' (kgf/cm²)	(3) $(\sigma_3')_f$ (kgf/cm²)	(4) $e_{0.3}$	(5) t_0 (mm)	(6) ϕ (degree)
1	0.02	0.060	0.680	0.1	44.3
2		0.038	0.689		43.9
3		0.057	0.714		42.0
4		0.048	0.722		41.5
5		0.033	0.754		40.3
6		0.034	0.769		39.8
7		0.030	0.833		37.5
8		0.026	0.900		35.6
9		0.038	0.679	0.3	47.2
10		0.033	0.755		43.4
11		0.051	0.853		38.4
12	0.05	0.070	0.687	0.1	43.7
13		0.061	0.722		42.4
14		0.064	0.782		39.0
15		0.063	0.833		37.4
16		0.058	0.908		35.4
17		0.066	0.687	0.12	44.6
18		0.065	0.761		41.1
19		0.067	0.681	0.3	45.4
20		0.065	0.739		42.4
21		0.056	0.898		37.9
22	0.10	0.117	0.686	0.1	43.7
23		0.115	0.758		40.4
24		0.103	0.902		35.4
25		0.118	0.687	0.12	43.9
26		0.117	0.740		41.2
27		0.107	0.902		35.6
28		0.120	0.650	0.3	46.0
29		0.122	0.687		44.9
30		0.108	0.696		44.3
31		0.110	0.773		41.1
32		0.110	0.824		39.2
33		0.118	0.866		38.0
34	0.20	0.213	0.658	0.3	43.9
35		0.215	0.664		45.0
36		0.218	0.669		44.5
37		0.215	0.718		42.3
38		0.213	0.734		40.9
39		0.213	0.746		40.5
40		0.212	0.771		39.8
41		0.210	0.775		39.7
42		0.211	0.827		38.1
43		0.202	0.885		37.1
44		0.209	0.888		36.6
45	0.50	0.514	0.658	0.3	43.3
46		0.514	0.693		42.2
47		0.513	0.727		40.3
48		0.513	0.750		39.5
49		0.512	0.788		38.0
50		0.512	0.831		36.1
51		0.511	0.881		34.4
52	1.0	1.014	0.653	0.3	42.4
53		1.015	0.671		42.3
54		1.013	0.723		40.1
55		1.013	0.730		40.1
56		1.013	0.731		39.7
57		1.015	0.760		38.4
58		1.013	0.764		38.0
59		1.013	0.803		36.4
60		1.012	0.806		36.9
61		1.012	0.811		36.8
62		1.012	0.829		35.5
63		1.012	0.853		35.2
64		1.012	0.878		34.4
65	2.0	2.013	0.655	0.3	41.5
66		2.012	0.677		40.5
67		2.014	0.713		39.4
68		2.014	0.720		39.7
69		2.013	0.749		38.1
70		2.013	0.781		37.0
71		2.012	0.829		35.3
72		2.010	0.876		34.1
73	4.0	not measured with a HC-DPT.	0.679	0.3	39.4
74			0.732		37.9
75			0.751		36.5
76			0.782		35.6
77			0.835		34.7
78			0.901		32.9

NOTE
(2) consolidation effective stress
(3) σ_3' at $(\sigma_1'/\sigma_3')_{max}$ measured with a high-capacity differential pressure transducer, uncorrected for membrane forces
(4) void ratio at $\sigma_c'=0.3$ kgf/cm²
(5) initial membrane thickness
(6) angle of internal friction, uncorrected for membrane forces

and minimum void ratio values are 0.977 and 0.605. The nominal values of diameter and height of specimen were 7 cm and 15 cm. Samples were prepared by the air pluviation method; air dry sand was pluviated through air from an nozzle of tube keeping the fall height constant. Densification of the samples was accomplished by increasing the fall height. The following cares were taken to maintain the accuracy of testing at low stresses.

(1) Both ends at the cap and at the pedestal were made of acryl platens having very smooth surfaces. These end surfaces

The Japanese Geotechnical Society

were well lubricated by using the method of so called Type 2 (Tatsuoka et al, 1984) where one layer of 50 μm-thick Shin-etsu silicone grease KS 63 G is placed between a 300 μm-thick latex disc and an acryl platen and this lubrication layer is doubled (in total two grease layers and two latex discs at each end). The angle of friction between a mass of Toyoura sand and this lubricated surface was found by direct shear tests to be around 0. 4 degree~0. 5 degree at a normal stress ranging from around 0. 25 kgf/cm^2 (25 kN/m^2) to around 6. 5 kgf/cm^2 (650 kN/m^2) (Tatsuoka et al, 1984). Shin-etsu silicone grease KS 63 G was selected because this kind of grease had been found very suitable for tests at relatively low normal stresses.

(2) Both the cap and the pedestal were enlarged (7. 5 cm in diameter compared to a diameter of sample of 7 cm) and the cap was fixed to the loading piston in order to have a uniform deformation of sample. Of course, it was confirmed before each test that the surfaces of cap and pedestal be parallel to each other.

(3) A membrane having an inner-diameter which was around 2 mm smaller than the inner-diameter of split mold was used to ensure a good fitting between the membrane and the inside surface of the mold when a vacuum was applied to the space between them. It was found from experiences that if these two kinds of diameters are similar, there may be a fold or folds in a membrane when the membrane is set in a mold and/or after a sample is consolidated. This arrangement induces an initial horizontal tensile strain of an order of 3% in the membrane. A membrane was set to a split mold in such that no initial axial strains induced in the membrane.

(4) After smoothing and flattering the sample surface by scraping with a thin wooden plate, the following procedures were employed in order not to disturb the sample: (a) The cap was placed with a seating stress of as small as around 3 gf/cm^2 (0. 3 kN/m^2). (b) The loading piston was clamped to the top portion of the bearing house. (c) The membrane was carefully sealed to the top cap in such that no membrane axial strain induced in it. (d) The loading piston was unclamped with keeping the seating stress to be 3 gf/cm^2. (e) The split collar was removed very carefully, which had been set on the top of the split mold in advance as shown in Fig. 2. It was considered that while the sample was not vacuumed yet at this moment most of the sand mass located between the bottom surface of the top acryl platen and the level of the top edge of the mold was not disturbed so much because the free gap was only 4 mm and some shear resistances might exist between the lubricated surface of the cap and the sample surface at a seating stress of 3 gf/cm^2. (f) A vacuum was applied to the sample with its value being 0. 02 kgf/cm^2 (1. 96 kN/m^2) for the sample which was sheared at this value of effective confining pressure (0. 02 kgf/cm^2). The vacuum value was 0. 05 kgf/cm^2 (4. 9 kN/m^2) for the sample sheared at an effective confining pressure of 0. 05 kgf/cm^2 or higher. It was confirmed that the top cap fell freely when the

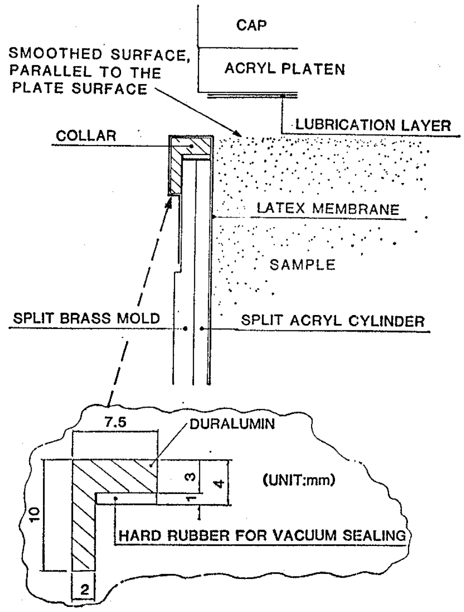

Fig. 2. Schematic diagram showing the condition just before seating of the cap on the sample surface

NII-Electronic Library Service

The Japanese Geotechnical Society

vacuum was applied because of the presence of the free gap made by removing the collar (Fig. 2). Note that in spite of the presence of this kind of gap the contact between the membrane and the inside surface of the mold may resist to some extent against the perfectly free axial deformation of sample when vacuuming. This kind of contact may disappear only after the sample is contracted to some extent in the radial direction, which will not be the case in the beginning stage of vacuuming. This is because the membrane is compressed radially to some extent even before the application of vacuum. Considering this above, it was decided to minimize the vacuum value to the smallest operational value as described above. But this value should be larger than the horizontal stress at the bottom of sample before the application of vacuum, which is only around 0.01 kgf/cm^2 (1 kN/m^2). (g) The split brass mold was carefully disassembled and the dimensions of sample were measured. For the sample sheared at an effective confining pressure of 0.5 kgf/cm^2 (49 kN/m^2) or higher, the vacuum was then increased to 0.3 kgf/cm^2 (29.4 kN/m^2) and the dimensions of sample were measured again.

(5) Samples were saturated by circulating sufficient amount of carbon-dioxide and de-air water through a specimen and applying a back pressure of 2.0 kgf/cm^2 (196 kN/m^2)

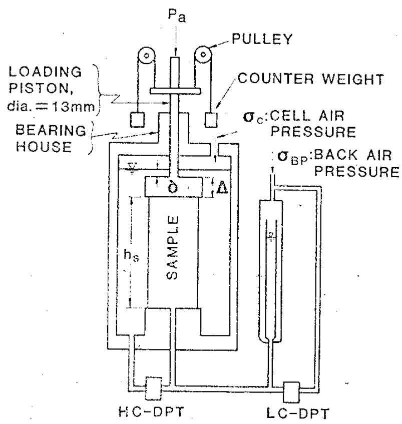

Fig. 3. Schematic diagram of triaxial compression test method for tests at an effective confining stress of 0.5kgf/cm^2 (49kN/m^2) or lower

for an effective confining stress σ_c' of 0.05 kgf/cm^2 (4.9 kN/m^2) or higher. When $\sigma_c'=0.02$ kgf/cm^2 (1.96 kN/m^2), no back pressure was applied in order not to disturb a sample during the application of back pressure. Back pressuring was considered necessary to measure accurately the volume change of sample by measuring the water height in burette. This water height was measured with a low-capacity differential pressure transducer (LC-DPT) as shown in Fig. 3 (Tatsuoka, 1981).

(6) To obtain the value of effective confining pressure or effective minor principal stress σ_3' during a triaxial compression test, the differential pressure between the cell water pressure and the pore water pressure was directly measured with a high capacity differential pressure transducer (HC-DPT) (Fuji Electric Co. Ltd, Model FFF-35) (see Fig. 3). The capacity of differential pressure for the HC-DPT was adjusted to an adequate value among 0.32 kgf/cm^2 (31.36 kN/m^2), 1.6 kgf/cm^2 (156.8 kN/m^2) and 3.2 kgf/cm^2 (313.6 kN/m^2). The estimated error in the measured differential pressure was around $\pm 0.3\%$ for the maximum differential pressure of 0.02 kgf/cm^2 (1.96 kN/m^2), which was mainly caused during the analog-to-digital conversion procedure in data acquisition. The error in percentage decreases with the increase in the measured differential pressure. Thus the value of σ_3' was calculated as

$$\sigma_3' = DP + \Delta\sigma_{rm} \qquad (1)$$

in which DP is the differential pressure as measured with the HC-DPT and $\Delta\sigma_{rm}$ is the stress correction for the forces working in membrane which will be described in detail later. Note that the value of DP is independent of the level where this is measured. Thus, when $\Delta\sigma_{rm}$ is independent of the level, σ_3' obtained by Eq. (1) is the same at any level in a sample.

(7) While the diameter of the loading piston was 20 mm for an effective confining pressure of 1 kgf/cm^2 (98 kN/m^2) or higher, this was reduced to 13 mm for an effective confining pressure of 0.5 kgf/cm^2 (49 kN/m^2)

NII-Electronic Library Service

The Japanese Geotechnical Society

or lower to reduce the piston friction. The loading piston was guided with two low-friction linear motion bearings in a bearing house located at the top plate of triaxial cell (Fig. 3). The sealing against pressurized cell air was achieved by placing a gap of 0.01 mm between the inside wall surface of the bearing house and the loading piston along a length of 5 cm between two bearings. For the tests at an effective confining pressure of 0.5 kgf/cm² (49 kN/m²) or lower, the combined weight of cap, loading piston and other attachments was counter-balanced as illustrated in Fig. 3 from the stage of contacting the cap with the top surface of sample in order to keep sample disturbances to the minimum. The total amount of friction against the upward or downward movement of the loading piston F_r was carefully evaluated under the actions of thrusting forces and was found not larger than 16 gf (0.16 N) which corresponds to an axial stress of as small as 0.4 gf/cm² (0.039 kN/m²) for the sample dimension employed in this study. The effective axial stress σ_1' at the mid-height of sample was calculated as

$$\sigma_1' = (P_a + W - F_r)/A_s + DP - [(\sigma_c + \delta \cdot \gamma_w)a + \Delta \cdot \gamma_w \cdot A_c]/A_s + (h_s/2) \cdot (G_s - 1)\gamma_w/(1+e) + \Delta\sigma_{a_m} \qquad (2)$$

in which P_a is the additional axial load measured with a load cell located at the top of the loading piston, W is the combined weight of cap, loading piston and other attachments ($W=0$ when counter-balanced), F_r is the loading piston friction, A_s and h_s are the cross-sectional area and the height of sample, DP is the differential pressure as measured, σ_c is the cell air pressure as measured with a pressure gage, δ is the cell water depth above the cap, Δ and A_c are the thickness and the cross-sectional area of cap, γ_w is the unit weight of water, a is the cross-sectional area of the loading piston, and $\Delta\sigma_{a_m}$ is the stress correction for membrane forces which will be described in detail later. The load cell was carefully calibrated very often by using dead weights.

(8) The axial displacement rate was as small as 0.25%/min so that no excess pore pressure be accumulated within a sample.

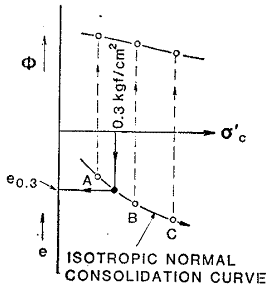

Fig. 4. Schematic diagram showing the change of ϕ along an identical isotropic normal consolidation curve

(9) All the values of stresses and strains were automatically recorded, processed and plotted by using a micro-computer in order to reduce the error during these steps.

In most cases, the density of each sample will be represented by the value of void ratio when the sample is isotropically consolidated at a pressure of 0.3 kgf/cm² (29.4 kN/m²), $e_{0.3}$ (see Fig. 4). The values of ϕ and several kinds of strain values will be compared among different samples having an identical value of $e_{0.3}$. In this sense, the changes of the values of ϕ or strain values with the change of pressure along an identical isotropic normal consolidation curve will be examined in this paper. The values of $e_{0.3}$ for samples which were sheared at stresses lower than 0.3 kgf/cm² such as Sample A as indicated in Fig. 4 were estimated by using the consolidation curves up to 0.3 kgf/cm² which were obtained for other samples having similar density values.

TYPICAL RECORDED STRESS AND STRAIN RELATIONS

The typical relationships between stress ratio σ_1'/σ_3', axial strain ε_a and volumetric strain v in a series of drained triaxial compression tests on samples having similar densities are shown in Figs. 5(a) and (b) and also in Figs. 5(c) and (d). Figs. 5(a) and (b) are on dense samples. Fig. 5(a) are for the samples consolidated to 0.1 kgf/

NII-Electronic Library Service

The Japanese Geotechnical Society

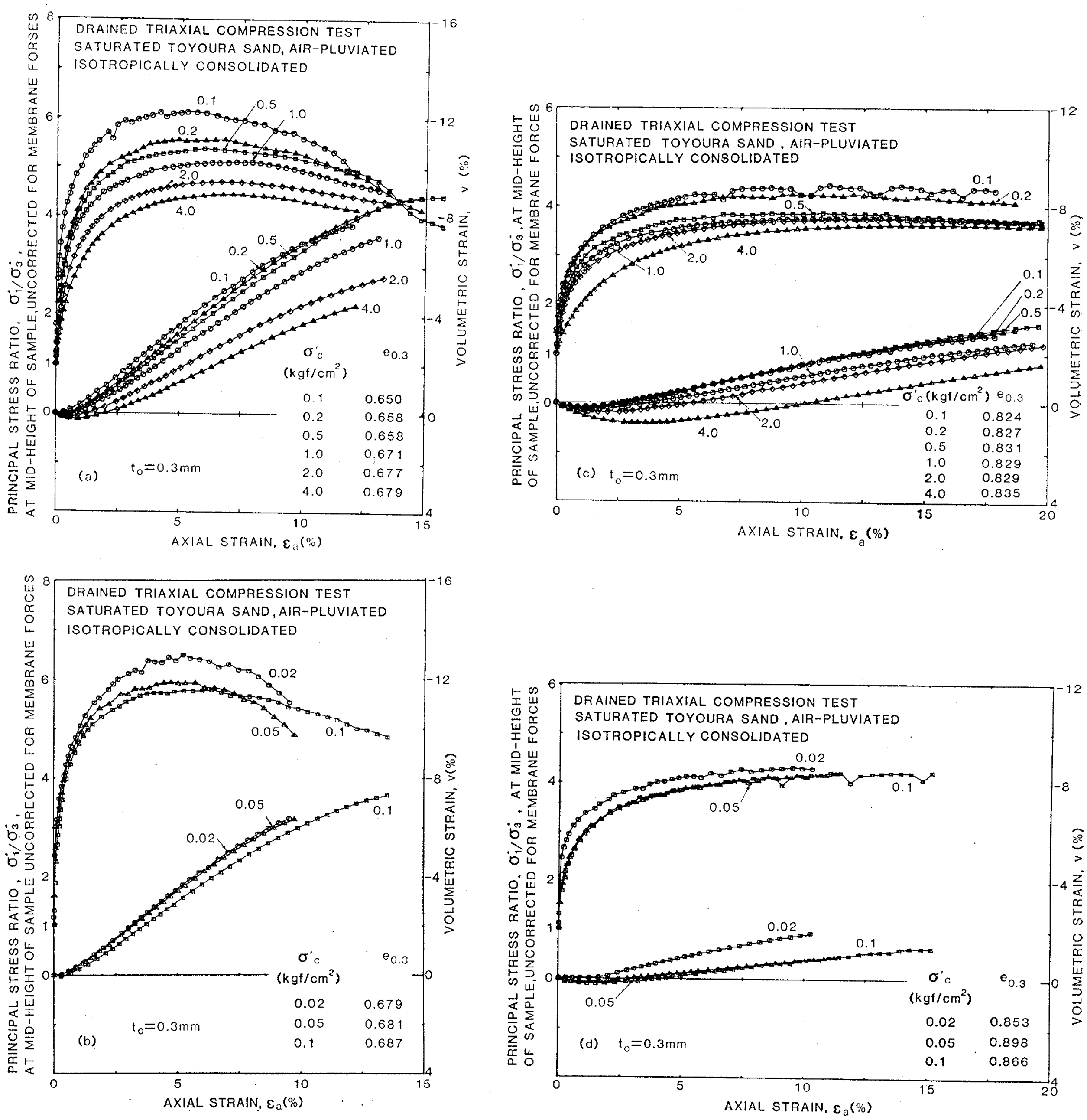

Fig. 5. Typical relationships between principal stress ratio at the mid-height of sample uncorrected for membrane forces, axial strain and volumetric strain for a membrane thickness of 0.3mm for (a) dense samples at $\sigma_c'=0.1\sim4$kgf/cm², (b) dense samples at $\sigma_c'=0.02\sim0.1$kgf/cm², (c) loose samples at $\sigma_c'=0.1\sim4$kgf/cm² and (d) loose samples at $\sigma_c'=0.02\sim0.1$kgf/cm² (1kgf/cm²=98kN/m²)

cm² (9.8 kN/m²) or higher and Fig. 5(b) are for those consolidated to 0.1 kgf/cm² or lower. Figs. 5(c) and (d) are similar ones for loose samples. Note that the membranes used for the data presented in Figs. 5(a) through (d) are latex rubber membranes having a Young's modulus of 15.2 kgf/cm² (1.49×10^3 kN/m²) and an initial averaged thickness t_0 of 0.3 mm. The stress values shown in these figures were those at the mid-height of sample without being corrected for membrane forces. It may be seen in these figures that for both cases, dense or loose, the change of the relationship between axial strain and uncorrected stress ratio σ_1'/σ_3' with the change of consolidation

NII-Electronic Library Service

The Japanese Geotechnical Society

pressure σ_c' becomes larger as σ_c' decreases while the change of the relationship between axial strain and volumetric strain with the change of σ_c' becomes smaller as σ_c' decreases. This apparently contradictory phenomenon will be explained in the following part by the effects of membrane forces on measured stresses.

Somewhat unsmooth stress and strain relations seen in Figs. 5(a) through (d) for extremely lower stresses ($\sigma_c' \leqq 0.1$ kgf/cm^2) can be considered due to their stick-slip behaviors. The angle of internal friction was defined for the maximum recorded or calculated stress ratio in any case in the following part whether stresses were corrected or uncorrected for membrane forces.

DEPENDENCY OF ANGLE OF INTERNAL FRICTION ON PRESSURE

The angles of internal friction ϕ obtained by using membranes having $t_0=0.3$ mm were calculated from the maximum stress ratio at the mid-height of sample without performing any stress corrections for membrane forces and plotted against the values of $e_{0.3}$ (Fig. 6). The figures indicated in Fig. 6 mean the values of minor principal stress at $(\sigma_1'/\sigma_3')_{max}$, $(\sigma_3')_f$, which have not been corrected for membrane forces either. The values of $(\sigma_3')_f$ were slightly different from the values of consolidation stress σ_c' at low stresses because of the unevitable changes of the surface levels of both cell water and water in burette and also because of the slight changes of both cell air pressure and back air pressure during a test. These kinds of changes were let to occur freely during tests because it was considered that the

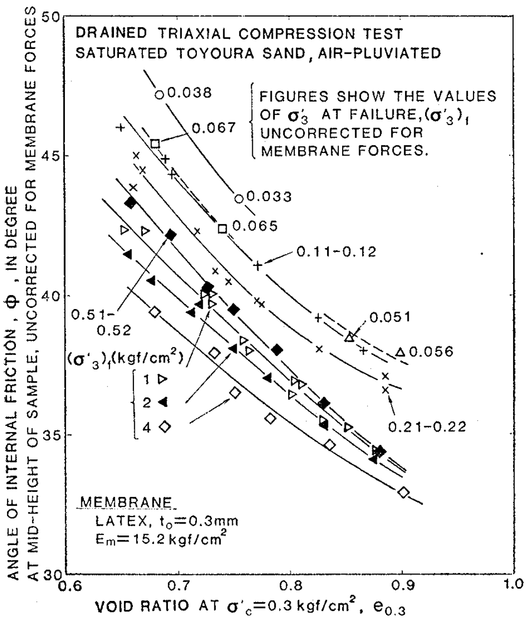

Fig. 6. Angle of internal friction at the mid-height of sample, uncorrected for membrane forces for $t_0=0.3$ mm, plotted against $e_{0.3}$ (1 kgf/cm^2=98 kN/m^2)

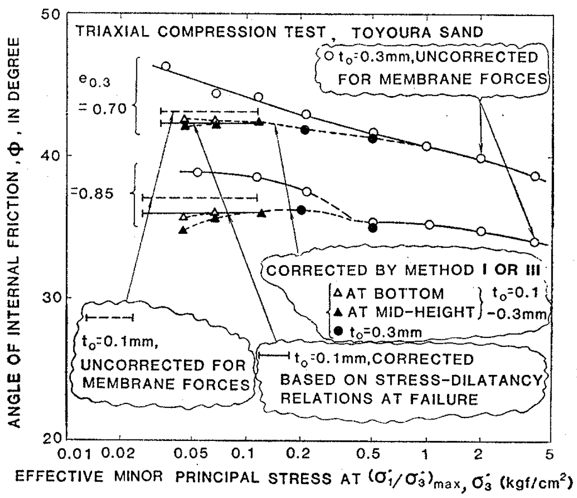

Fig. 7. Relationship between angle of internal friction obtained by various methods and effective minor principal stress at failure in logarithmic scale (1 kgf/cm^2=98 kN/m^2)

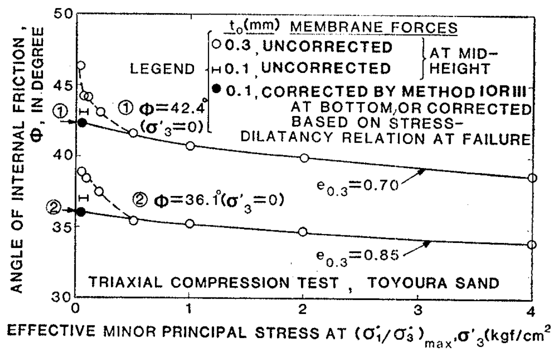

Fig. 8. Relationship between angle of internal friction obtained by various methods and effective minor principal stress at failure in arithmetic scale

NII-Electronic Library Service

The Japanese Geotechnical Society

adjustments might induce more variations in σ_3' than it was in the case of no-adjustment. It may be seen in this figure that the scattering among the data is very small even when $(\sigma_3')_f$ is as low as 0.2 kgf/cm^2 or lower.

Since the relationships between ϕ and $e_{0.3}$ could be well defined for each stress level, the values of ϕ for $e_{0.3}=0.70$ or $e_{0.3}=0.85$ were read for each stress level and plotted against $(\sigma_3')_f$ both in the logarithmic scale (Fig. 7) and in the arithmetic scale (Fig. 8). At least two important points may be seen from these figures. First, the true values of ϕ at lower stresses should be smaller than those indicated by the hollow circles especially at σ_3' lower than 0.1 kgf/cm^2 (9.8 kN/m^2) because the errors due to the effects of membrane forces for a rather thick membrane of $t_0=0.3$ mm involved in these data always increase the calculated values of ϕ. In spite of this fact, it may be seen that the rate of the change of ϕ with the change of σ_3' in this case is much smaller than that indicated in Figs. 1(a) and (b). The reason for this apparent difference can not be explained by the present authors mainly because several experimental details for the data shown in Figs. 1(a) and (b) are not presented in the literature.

Second, it may be seen from Fig. 7 that in the case of $e_{0.3}=0.85$ the manner of the change of ϕ with the change of σ_3' when σ_3' is between 0.5 kgf/cm^2 (49 kN/m^2) and 0.2 kgf/cm^2 (19.2 kN/m^2) is not smooth, but is rather unnatural. This may be due to that at σ_3' lower than 0.5 kgf/cm^2 the effects of membrane forces are especially larger for these looser samples having $e_{0.3}=0.85$ than for denser samples because the maximum value of σ_1'/σ_3' is attained at a larger strain value for a looser sample, resulting in larger membrane forces. This trend may also indicate the necessity of stress corrections for membrane forces at least for the case of $t_0=0.3$ mm.

In view of the above, additional drained triaxial compression tests on specimens consolidated to an effective consolidation

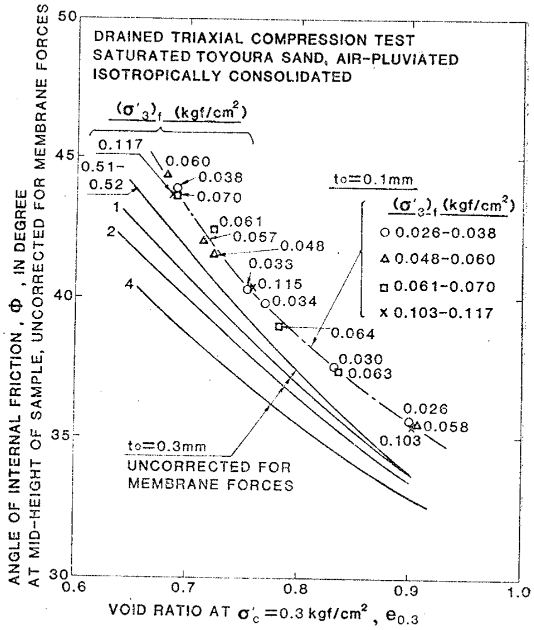

Fig. 9. Angle of internal friction at the mid-height of sample, uncorrected for membrane forces for t_0=0.1mm, plotted against $e_{0.3}$ (1 kgf/cm^2=98 kN/m^2)

pressure σ_c' of 0.1 kgf/cm^2 (9.8 kN/m^2) or lower were performed using thinner latex membranes having $t_0=0.1$ mm or 0.12 mm. The uncorrected values of ϕ at the mid-height of samples when $t_0=0.1$ mm were plotted against $e_{0.3}$ (Fig. 9). The figures indicated in Fig. 9 are the values of effective minor principal stress at $(\sigma_1'/\sigma_3')_{max}$, $(\sigma_3')_f$, which have not been corrected for membrane forces either. Since no clear effects of $(\sigma_3')_f$ on the values of ϕ could be seen among the data, the values of ϕ for $e_{0.3}=$ 0.70 and 0.85 were read from these data and indicated in Fig. 7 by two horizontal broken lines, which were determined as $\phi=43$ degrees for $(\sigma_3')_f=0.038\sim0.117$ kgf/cm^2 (3.7$\sim$11.5 kN/m^2) and $\phi=37$ degrees for $(\sigma_3')_f=0.026\sim0.103$ kgf/cm^2 (2.5$\sim$10.1 kN/m^2). It may be seen from Fig. 7 that when stresses are not corrected for membrane forces the calculated values of ϕ are smaller for $t_0=0.1$ mm than for $t_0=0.3$ mm, with the difference increasing with the decrease in σ_3' or $(\sigma_3')_f$. This is also another evidence for the effects of membrane forces on the measured value of ϕ.

NII-Electronic Library Service

The Japanese Geotechnical Society

If the effects of membrane forces are not negligible in obtaining the true values of ϕ at σ_3' lower than around 0.1 kgf/cm^2 even when thin membranes having an initial thickness $t_0=0.1$ mm are used, another important conclusion may be derived from the data shown in Fig. 9. If the values of ϕ indicated in Fig. 9 are properly corrected for membrane forces, the corrected values of ϕ will decrease. The amount of decrease will increase as $(\sigma_3')_f$ decreases because the effects of membrane forces on the values of ϕ are larger for lower values of $(\sigma_3')_f$. Then, the corrected values of ϕ become smaller with the decrease in σ_3' when σ_3' is lower than around 0.1 kgf/cm^2 (10 kNm^2). This conclusion seems rather unnatural. However, it is to be noted that the stress condition within a sample becomes very non-uniform at extremely low pressures. The values of ϕ indicated in Fig. 9 were calculated from the maximum stress ratio value $(\sigma_1'/\sigma_3')_{max}$ at the mid-height of sample. For example, suppose that at the mid-height of sample the true stress values are $(\sigma_3')_f=$ 0.045 kgf/cm^2 (4.41 kN/m^2) and $(\sigma_1')_{max}=$ 0.227 kgf/cm^2 (22.2 kN/m^2), resulting in $(\sigma_1'/\sigma_3')_{max}=5.045$ or $\phi=42.0$ degrees. When the void ratio value e is 0.7, the value of $(\sigma_1')_{max}$ at the bottom becomes 0.2342 kgf/cm^2 (22.95 kN/m^2). When the effects of membrane forces on the value of $(\sigma_3')_f$ are the same at any level in the sample and also the horizontal shear stress working on the bottom surface of sample can be neglected, the value of $(\sigma_3')_f$ at the bottom of sample is also 0.045 kgf/cm^2. Then, the value of $(\sigma_1'/\sigma_3')_{max}$ at the bottom of sample becomes 5.20, giving $\phi=42.7$ degrees, which is 0.7 degrees larger than the value of ϕ calculated from the stress values at the mid-height of sample. Therefore, it can be said that if the failure of sample is controlled by the maximum value of $(\sigma_1'/\sigma_3')_{max}$ within a sample, the values of ϕ obtained from the stresses at the mid-height of sample are underestimated ones especially at lower stresses even if stresses have been properly corrected for membrane forces. Therefore, it seems that the trend indicated in Fig. 9 be quite possible. This point will be discussed again later.

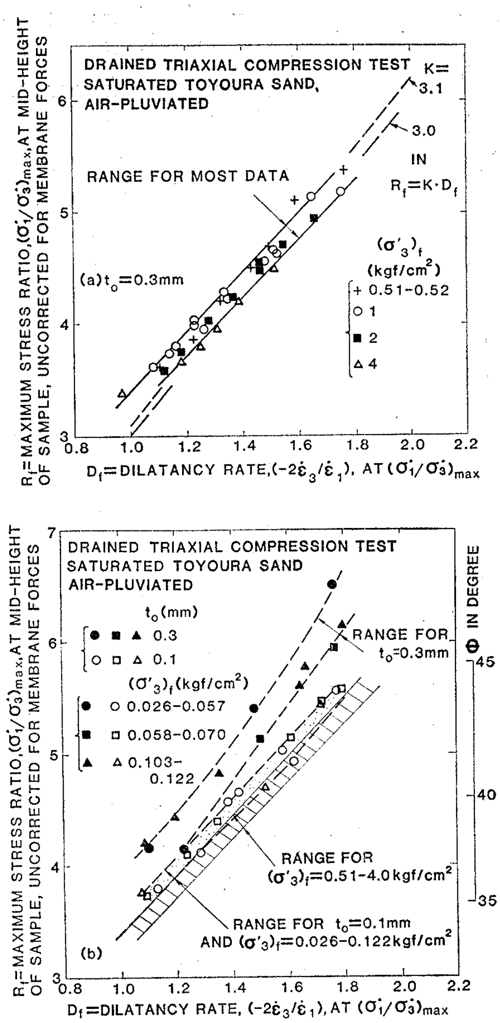

Fig. 10. Stress-dilatancy plottings at failure at (a) $\sigma_3'=0.51\sim4$ kgf/cm^2 and (b) $\sigma_3'=0.026\sim0.122$ kgf/cm^2, with stress values as follows being uncorrected for membrane forces (1 kgf/cm^2=98 kN/m^2)

In an attempt to know the extent of the effects of membrane forces on measured values of ϕ, another kind of analysis was performed as follows. In Fig. 10(a) are shown the stress-dilatancy plottings at failure for $(\sigma_3')_f=0.51\sim4.0$ kgf/cm^2(50.0$\sim$392 kN/m^2) where the membrane forces have only negligible effects on measured values of $(\sigma_1'/\sigma_3')_{max}$. While a small scattering can be seen among the data, the relations can be considered quite independent of the value of $(\sigma_3')_f$. In Fig. 10(b) are shown the

NII-Electronic Library Service

The Japanese Geotechnical Society

similar stress-dilatancy plottings at failure for $(\sigma_3')_f=0.026\sim0.122$ kgf/cm^2 (2.5~12.0 kN/m^2) for two membrane thickness values, $t_0=0.1$ mm and 0.3 mm. The range for $(\sigma_3')_f=0.51\sim4$ kgf/cm^2 is also indicated in Fig. 10(b). Note that the values of $(\sigma_1'/\sigma_3')_{\max}$ and $(\sigma_3')_f$ indicated in Fig. 10(a) and (b) are the ones uncorrected for membrane forces, measured at the mid-height of sample. It may be clearly seen in Fig. 10(b) that the data points for $t_0=0.3$ mm are located quite higher than those for $t_0=0.1$ mm which are in turn located slightly higher than those for $(\sigma_3')_f=0.51\sim4$ kgf/cm^2. If the stress-dilatancy relation at failure is independent of the value of $(\sigma_3')_f$ for the range of σ_3' between 0.026 kgf/cm^2 (2.5 kN/m^2) and 4.0 kgf/cm^2 (392 kN/m^2), we can conclude from the data shown in Fig. 10 (b) that for both $t_0=0.3$ mm and 0.1 mm the effects of membrane forces should be accounted for to obtain the true values of ϕ, with the correction being larger for $t_0=0.3$ mm than for $t_0=0.1$ mm.

STRESS CORRECTION FOR MEMBRANE FORCES

The shape of membrane during a triaxial compression test at low stresses is rather complicated because of very rough surfaces of sand samples and also because the buckling of membrane can occur at a larger axial strain especially at extremely low pressures. By these reasons, it is very difficult to find an exact method of stress corrections for membrane forces for sand specimens. Therefore, the following three methods were compared.

Method I : In this method, it is assumed that a membrane has a shape of perfect thin-wall cylindrical shell. Thus this method was called "Compression shell theory" by Henkel and Gilbert (1952). The stress corrections for membrane forces are expressed on the theory of elasticity as

$$\Delta\sigma_{a_m}=-(8/3)[E_m\cdot t(2\varepsilon_{a_m}+\varepsilon_{\theta_m})]/d$$
$$\Delta\sigma_{r_m}=-(4/3)[E_m\cdot t(\varepsilon_{a_m}+2\varepsilon_{\theta_m})]/d \quad (3)$$

in which $\Delta\sigma_{a_m}$ and $\Delta\sigma_{r_m}$ are the corrections to the axial and radial stresses (refer to Eqs. (1) and (2)), E_m and t are the Young's modulus and the present averaged thickness of membrane, d is the present diameter of sample and ε_{a_m} and ε_{θ_m} are the averaged axial and circumferential strains in membrane which were assumed equal to the averaged axial and radial strains in a sample in this study. Of course the values of ε_{a_m} and ε_{θ_m} were obtained accounting for initial strains in membranes. Note that a Poisson's ratio of 0.5 is used to derive Eq. (3) and will also be used in the following two methods. Eq. (3) or similar ones with slight modifications has been used by many researchers; for clay samples by Henkel and Gilbert (1952), Duncan and Seed (1967) and Berre (1982) and for sand samples by Ponce and Bell (1971) and Molenkamp and Luger (1981).

Method II : It is assumed that in a membrane the axial deformation occurs independently of the radial and circumferential deformations. The equations for stress corrections are

$$\Delta\sigma_{a_m}=-(4E_m\cdot t\cdot\varepsilon_{a_m})/d$$
$$\Delta\sigma_{r_m}=-(2E_m\cdot t\cdot\varepsilon_{\theta_m})/d \quad (4)$$

Method III : In this method it is assumed that the resistance of membrane against axial deformation is negligible due to such a buckling phenomenon as schematically illustrated in Fig. 11 which is assumed to occur over the whole area of membrane. This method was called "Hoop tension theory" by Henkel and Gilbert (1952). The

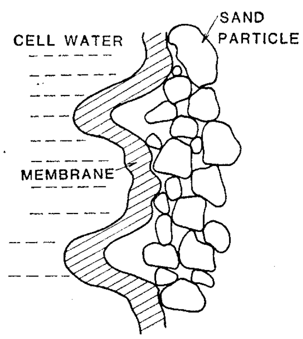

Fig. 11. Schematic diagram of buckling of membrane

NII-Electronic Library Service

The Japanese Geotechnical Society

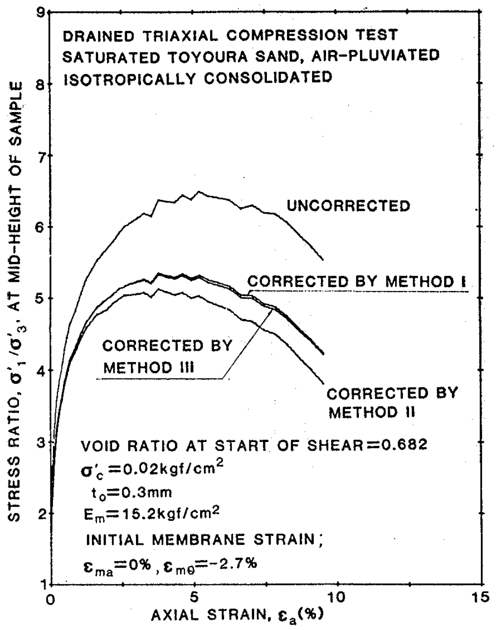

Fig. 12. Stress-strain relationships for stresses corrected or uncorrected for membrane forces ($1\,\mathrm{kgf/cm^2}=98\,\mathrm{kN/m^2}$)

equations for stress corrections, which are slightly different from the equations shown by Henkel and Gilbert, are

$$\Delta\sigma_{a_m}=0,\quad \Delta\sigma_{r_m}=-(2E_m\cdot t\cdot\varepsilon_{\theta_m})/d \qquad (5)$$

In Fig. 12 are shown the relationships between axial strain and principal stress ratio at the mid-height of sample which are either uncorrected or corrected for membrane forces by these three methods for a sample consolidated to $\sigma_c'=0.02\,\mathrm{kgf/cm^2}$ ($1.96\,\mathrm{kN/m^2}$). Of course, the initial strains of the membrane were accounted for, which are $(\varepsilon_{a_m})_i=0.0\%$ and $(\varepsilon_{\theta_m})_i=-2.7\%$. It may be seen in Fig. 12 that the stress corrections for membrane forces are quite large when the confining stress is extremely low and a thick membrane ($t_0=0.3$ mm) is used. It may also be seen that the corrected stress values are different between Method II and the other correction methods (Methods I and III). Since Method II is rather unrealistic from the viewpoint of the elasticity theory, this method will not be considered anymore in this paper.

It may also be seen in Fig. 12 that Methods II and III provide very similar stress values,

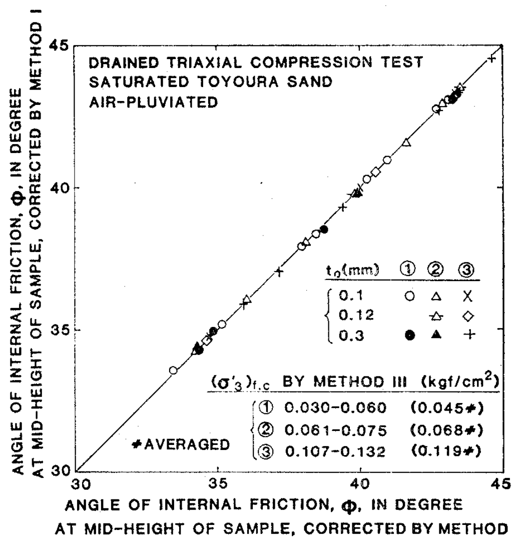

Fig. 13. ϕ **corrected by Method I versus** ϕ **corrected by Method III for** σ_c' **equal to or less than** $0.1\,\mathrm{kgf/cm^2}$ ($9.8\,\mathrm{kN/m^2}$)

while in these methods quite different modes of deformation of membrane are considered. In Fig. 13 are plotted the corrected values of ϕ at the mid-height of sample obtained by Method I against those by Method III for all the tests performed at $\sigma_c'=0.1\,\mathrm{kgf/cm^2}$ ($9.8\,\mathrm{kN/m^2}$) or lower. It may be seen that the difference of ϕ between these two methods are very small. In particular, the difference is not larger than around 0.1 degree when $t_0=0.1$ mm, which is of a similar order of the estimated error in this study. This result seems only to be fortuitous, because Method I and Method III may provide different results, for example, in constant-volume tests on sands or in drained tests on non-dilative soils such as normally consolidated clay. This is because in these tests the volumetric strains can be much less than the radial strains, resulting in different corrections to radial stress between Methods I and III.

In Fig. 14 (a) are shown the angles of internal friction ϕ calculated by using the stresses at the mid-height of sample, which are either uncorrected or corrected for membrane forces by two methods (Methods I and III), obtained for the samples consolidated to $\sigma_c'=0.02\,\mathrm{kgf/cm^2}$, using two kinds of membrane thickness, $t_0=0.1$ mm and 0.3

NII-Electronic Library Service

The Japanese Geotechnical Society

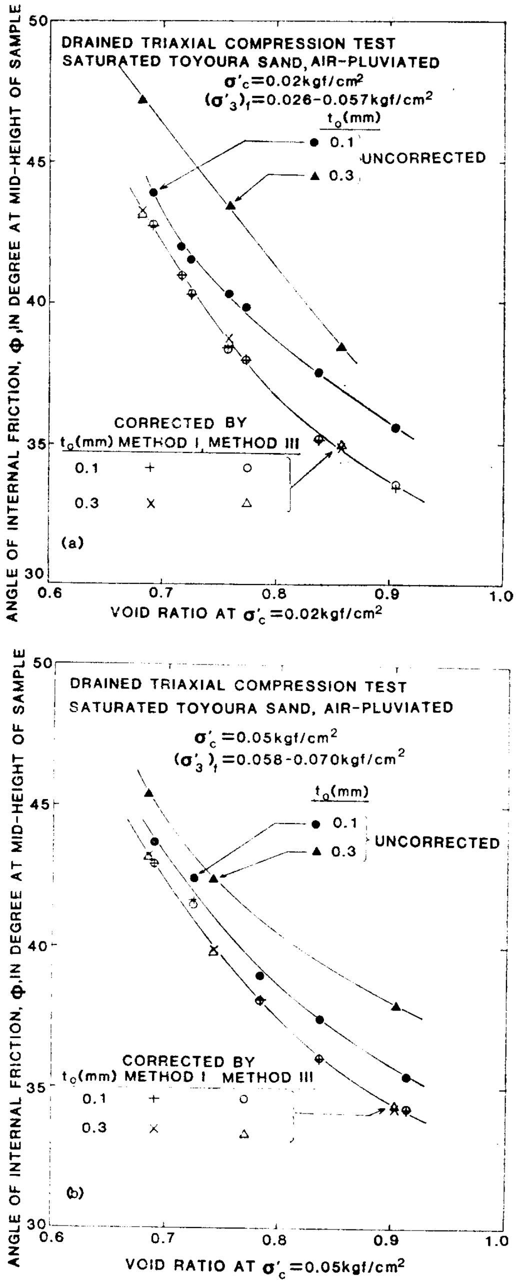

Fig. 14. Angles of internal friction, uncorrected or corrected for membrane forces for samples consolidated to (a) $\sigma_c'=0.02$ kgf/cm^2 and (b) $\sigma_c'=0.05$ kgf/cm^2 (1 kgf/cm^2=98 kN/m^2)

mm. Also in Fig. 14(b) are shown the angles of internal friction for the samples consolidated to $\sigma_c'=0.05$ kgf/cm^2. It may be seen in Figs. 14 (a) and (b) that the values of ϕ corrected by either Method I or Method III are very similar between for $t_0=0.1$ mm and for $t_0=0.3$ mm. Accordingly, both Method I and Method III can be considered appropriate for the membrane force correction at peak stress conditions for the test condition employed in this study or for similar conditions.

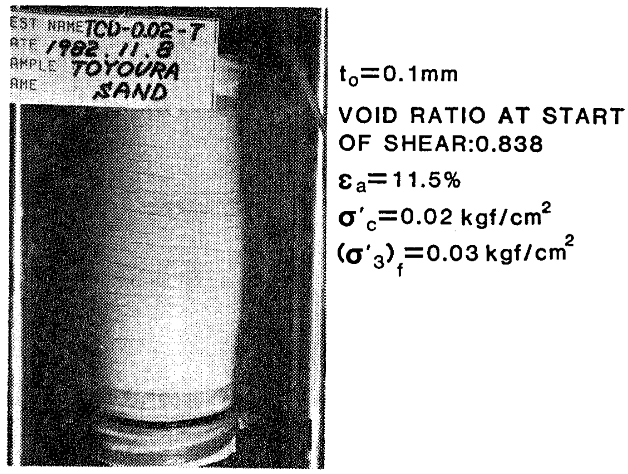

Photo. 1. Shape of sample vacuumed after test which stopped at $\varepsilon_a=11.5\%$

It was observed in the tests at extremely low pressures that membranes did not buckle at small axial strains, where dense samples had their peak stress values, while most membranes buckled at larger axial strains, where loose samples had their peak stress values as typically shown in Photo. 1. Many horizontal lines seen on the surface of sample in Photo. 1 are the results of bucklings of membrane. In physical terms, it seems that Method I is more reasonable than Method III at smaller axial strains, while Method III is more reasonable than Method I at larger axial strains. Since any clear difference in the corrected values of ϕ between these two methods was not seen in this study for both dense and loose samples, both methods will be used together in the following part. Of course, it is likely that both Method I and III are still not the perfect ones due to many reasons as described later.

In Figs. 15(a) and (b) are shown the summaries of the angles of internal friction ϕ corrected by (a) Method I and (b) Method III obtained for three kinds of membrane thickness, $t_0=0.1$ mm, 0.12 mm and 0.3 mm for three ranges of stress, $(\sigma_3')_{f,c}$, which is

NII-Electronic Library Service

The Japanese Geotechnical Society

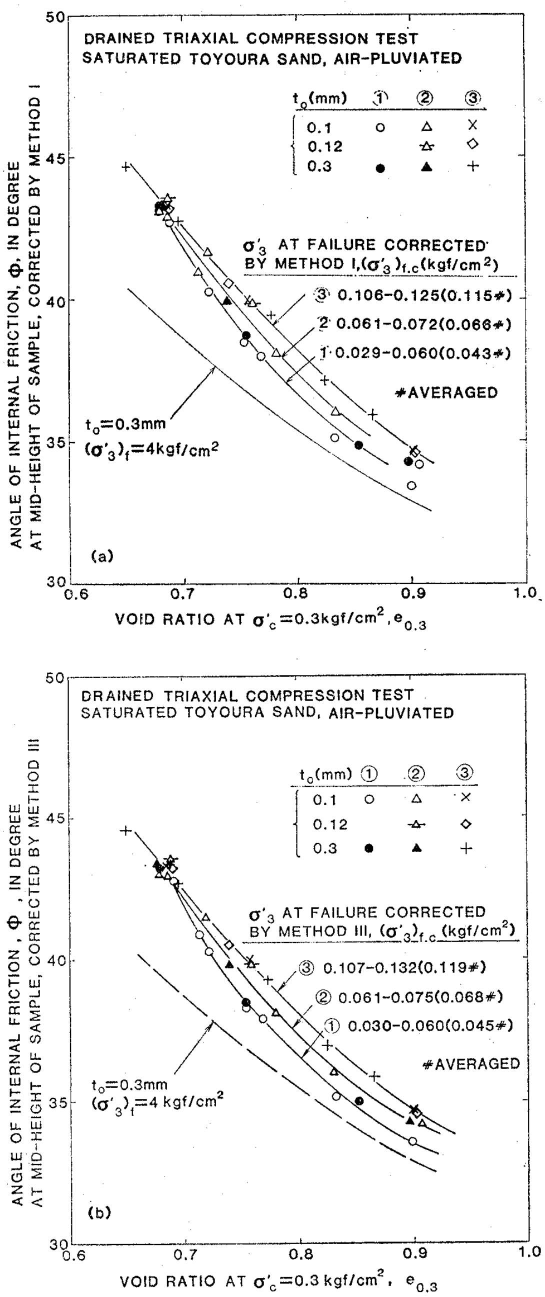

Fig. 15. Angles of internal friction corrected for membrane forces by (a) Method I and (b) Method III for t_0=0.1mm, 0.12mm and 0.3mm for σ_c' equal to or less than 0.1kgf/cm^2

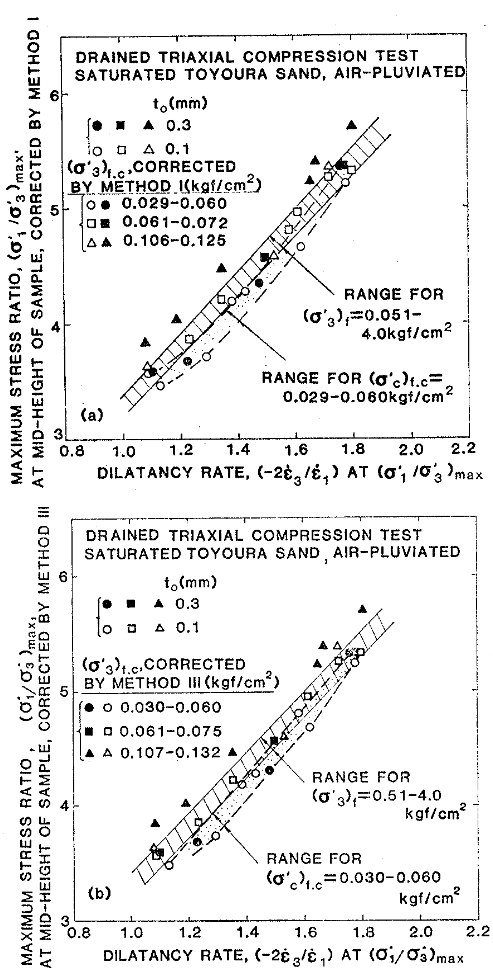

Fig. 16. Stress-dilatancy plottings at failure for stress ratio at the mid-height of sample corrected for membrane forces by (a) Method I and (b) Method III at extremely low pressures as compared with that at $(\sigma_3')_f$=0.51~4.0kgf/cm^2 (1kgf/cm^2=98kN/cm^2)

the minor principal stress at failure corrected for membrane forces. It may be seen that for any stress range the membrane thickness t_0 has no clear effects on the value of ϕ when stresses are corrected for membrane forces. The values of ϕ for $e_{0.3}$=0.70 and 0.85 were read from the relations shown in Figs. 15(a) and (b) and plotted in Fig. 7 using the averaged value of $\sigma_3=(\sigma_3')_{f.c}$ for each stress range indicated in Figs. 15(a) and (b), without distinguishing these two methods. Solid circles shown in Fig. 7 represent the values of ϕ for t_0=0.3 mm corrected by either Method I or Method III obtained for the samples consolidated to σ_c'=0.2 kgf/cm^2 and 0.5 kgf/cm^2. It may be seen in Figs. 7 and 15 that the values of ϕ obtained from the stress values at the mid-height of sample corrected by either Method I or Method III becomes smaller as σ_3' decreases when σ_3' is lower than around 0.1 kgf/cm^2. This trend may be due to an

NII-Electronic Library Service

The Japanese Geotechnical Society

underestimation of ϕ at lower values of σ_3'.

To confirm this point, the stress-dilatancy relations at failure were plotted in Figs. 16(a) and (b) where stress values were the ones at the mid-height of sample, corrected by (a) Method I and (b) Method III, obtained at $(\sigma_3')_{f.c}$ equal to (a) 0.125 kgf/cm^2 (12.3 kN/m^2) or lower or (b) 0.132 kgf/cm^2 (12.9 kgf/cm^2) or lower. It may be seen in both Figs. 16(a) and (b) that while there is a scattering among the data, the data points for $(\sigma_3')_{f.c}$ less than 0.060 kgf/cm^2 (5.9 kN/m^2) are located slightly below the range for $(\sigma_3')_f=0.51\sim4.0$ kgf/cm^2 (50~392 kN/m^2). This may indicate that when the effects of $(\sigma_3')_f$ on the true stress-dilatancy relations at failure are negligible for the range of $(\sigma_3')_f$ between 0.029 kgf/cm^2 (2.8 kN/m^2) and 4.0 kgf/cm^2 (392 kN/m^2), at least the values of $(\sigma_1'/\sigma_3')_{max}$ for $(\sigma_3')_{f.c}$ less than 0.060 kgf/cm^2 (5.9 kN/m^2) indicated in Figs. 16 (a) and (b) are slightly underestimated ones in obtaining the true angle of internal friction.

In view of the above, the value of $(\sigma_1'/\sigma_3')_{max}$ at the bottom of sample were calculated accounting for the self-weight of sample assuming that the value of σ_3' is the same at any level in a sample as described before. Then, the angles of internal friction were calculated from these values of $(\sigma_1'/\sigma_3')_{max}$. These values are indicated by hollow triangles in Fig. 7 and solid circles in Fig. 8. The relationships between ϕ and σ_3' thus obtained look smoother and more natural than the others. Probably, these relations are very close to the true relations. However, these relations may still involve some, probably very small, errors due to the following causes. First, when a sample is long with the initial height to diameter ratio of 2.1 as in this study it does not deform as a right cylinder even with the well lubricated ends, while the shape is more closer to a right cylinder than that in the case of tests using regular or non-lubricated ends. Furthermore, the horizontal shear stress at the top and bottom of sample is not perfectly zero due to both imperfect lubrication and the forces working in the end latex discs. In adition to these, in Method I, since the shape of the membrane even before buckling is not of perfect thin wall cylinder shell as assumed, Eq. (3) may not be an exact one. Also in Method III, since the manner of buckling of membrane when it occures is not as perfect as assumed, the resistance of membrane against axial deformation may not be perfectly zero. It was considered not capable for the present authors to obtain the truly exact stress condition within a sample which is needed to obtain the true value of ϕ at extremely low stresses. Further researches will be necessary to clarify this point.

Another independent attempt was made to correct the stress values for membrane forces. It was assumed that the differences in the locations of the stress-dilatancy plottings among the data for different stress ranges presented in Fig. 10(b) are caused only by the errors in measured stress values. The stress ratio values $(\sigma_1'/\sigma_3')_{max}$ for $t_0=0.1$ mm and at $(\sigma_3')_f=0.026\sim0.122$ kgf/cm^2 (2.5~12.0 kN/m^2) were reduced in such that the range of these data overlapped the range for $(\sigma_3')_f=0.51\sim4$ kgf/cm^2. The values of ϕ at $e_{0.3}=0.70$ and 0.85 for $t_0=0.1$ mm were obtained from the values of $(\sigma_1'/\sigma_3')_{max}$ corrected as above and these reduced values of ϕ were indicated by two solid horizontal lines in Fig. 7 and two solid circles in Fig. 8. The ranges of σ_3' for these lines shown in Fig. 7 were taken to be the same with the ranges for the broken lines expediently. It may be seen in Fig. 7 that the values of ϕ thus obtained are quite similar to those values of ϕ obtained from the values of $(\sigma_1'/\sigma_3')_{max}$ at the bottom of sample with being corrected for membrane forces by either Method I or Method III.

In summary, it may be concluded that the true value of ϕ at extremely low values of σ_3' lower than around 0.1 kgf/cm^2 (10kN/m^2) may be very close to either the values obtained from the values of $(\sigma_1'/\sigma_3')_{max}$ at the bottom of sample corrected

NII-Electronic Library Service

The Japanese Geotechnical Society

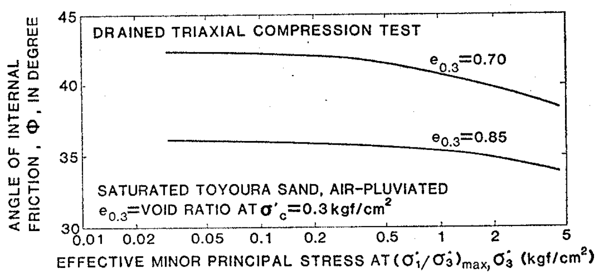

Fig. 17. Summarized relationships between ϕ and σ_3' for $e_{0.3}=0.70$ and 0.85 (1kgf/cm^2=98kN/m^2)

for membrane forces by either Eq. (3) (Method I) or Eq. (5) (Method III) or the values obtained by the correction method based on the stress-dilatancy relations at failure. The curves shown in Fig. 17 were obtained by averaging two relations obtained by these two methods above. It may be seen that the change of ϕ with the change of σ_3' is quite small when σ_3' is lower than around 0.5 kgf/cm^2 (49 kN/m^2). In particular, there is almost no change in the value of ϕ when σ_3' is lower than around 0.1 kgf/cm^2 (10 kN/m^2).

Another important conclusion may be obtained from Fig. 8. The relationships between ϕ and σ_3' represented by two solid curves shown in Fig. 8 correspond to those shown in Fig. 17. From these curves, the values of ϕ at $\sigma_3'=0.0$ can be reasonably obtained by extrapolating these curves to the points of $\sigma_3'=0.0$, which are $\phi=42.4$ degrees for $e_{0.3}=0.70$ and $\phi=36.1$ degrees for $e_{0.3}=0.85$. This indicates that it is not necessary to introduce the apparent cohesion intercept when the Mohr-Coulomb theory is used for the data obtained by this investigation. Furthermore, it may be seen in Fig. 8 that when σ_3' is represented in the arithmetic scale the rate of the change of ϕ with the change of σ_3' does not change so much as σ_3' changes.

It seems that these conclusions can simplify the analyses of model test results, because these results suggest that the angle of internal friction within a uniform model sand ground or slope is not needed to change or is needed to change only slightly at different depths. Of course, due to the anisotropic nature of strength of sand the value of ϕ may change with depth if the directions of principal stresses changes with depth. This point is beyond the scope of this paper. The reason for very small or negligible dependency of ϕ on the value of σ_3' at extremely low pressures for Toyoura sand is not clarified yet. Further researches will be needed.

DEFORMATION CHARACTERISTICS AT EXTREMELY LOW PRESSURES

It may be seen from Figs. 5(a) through

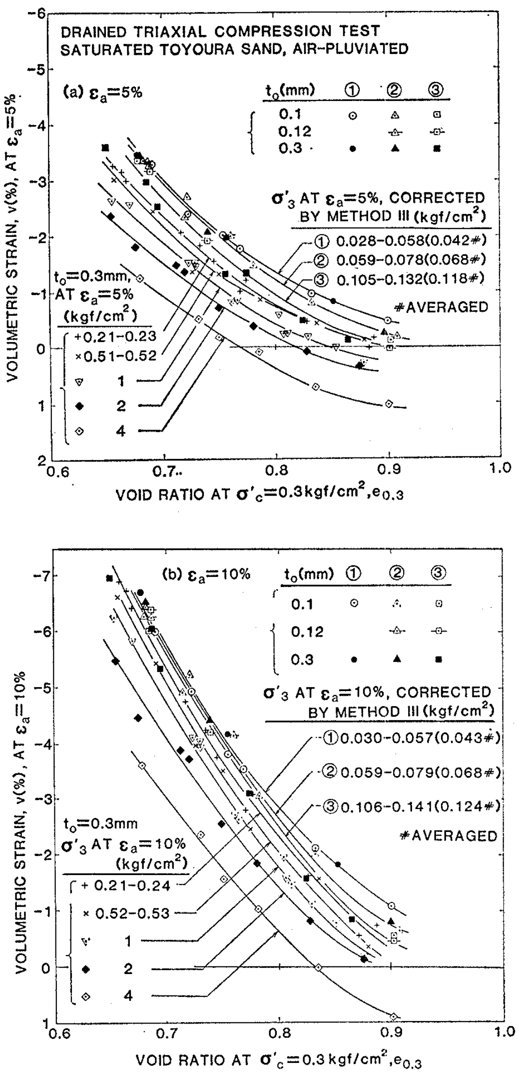

Fig. 18. Volumetric strain values at (a) $\varepsilon_a=5\%$ and (b) $\varepsilon_a=10\%$ versus void ratio $e_{0.3}$ (1kgf/cm^2=98kN/m^2)

NII-Electronic Library Service

The Japanese Geotechnical Society

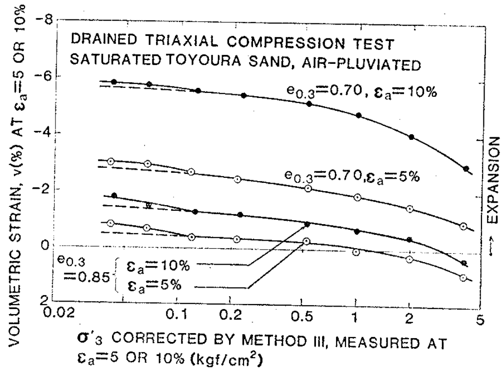

Fig. 19. Volumetric strain values at ε_a=5% or 10% versus σ_3' for $e_{0.3}$=0.70 and 0.85 (1kgf/cm^2=98kN/m^2)

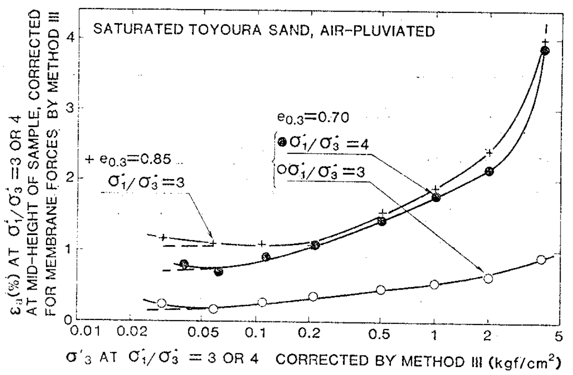

Fig. 20. Axial strain values at σ_1'/σ_3'=3 or 4 versus σ_3' for $e_{0.3}$=0.70 and 0.85 with stresses being corrected for membrane forces by Method III(1kgf/cm^2=98kN/m^2)

(d) that the volumetric strain-axial strain curves show small differences at different confining pressures when σ_c' is around 0.1 kgf/cm^2 or lower, while at higher stresses this difference increases with the increase in confining pressure. In Figs. 18(a) and (b) are plotted the values of volumetric strain v at an axial strain ε_a of 5% or 10% against the values of $e_{0.3}$. Any corrections to measured values of ε_a and v were not made for bedding errors for the data shown in Figs. 18(a) and (b) and the following figures. Since rather large strain values are presented in these figures, it can be considered that the effects of bedding error on the relationships shown in these figures be rather small. Also it was considered that the volume change due to the change of effective confining pressure during triaxial compression be negligible. It may be seen that for the data when $(\sigma_3')_f$ equals 0.1 kgf/cm^2 or lower the effects of membrane thickness on the values of v are negligible. In Fig. 19 are plotted the values of v at ε_a=5% or 10% for $e_{0.3}$=0.70 and 0.85 obtained from the relations indicated in Figs. 18(a) and (b). It may be seen that the trends of the change of v with the change of σ_3' are very similar to those for ϕ shown in Fig. 17. Furthermore, in Fig. 20 are shown the relationship between axial strain values observed at σ_1'/σ_3'=3 or 4 and σ_3' which were obtained by the procedure similar to that used to make Fig. 19. In Fig. 20, the value of σ_1'/σ_3' and σ_3' are those at the mid-height of sample corrected for membrane forces by Method III. It may be seen in Fig. 20 that the changes of the value of ε_a thus defined with the change of σ_3' are virtually smaller when σ_3' is less than around 0.5 kgf/cm^2 (50 kN/m^2), especially when σ_3' is less than around 0.1 kgf/cm^2 (10 kN/m^2). This trend seems to correspond very well to that seen in both Figs. 17 and 19. These results shown in Figs. 19 and 20 may support the conclusions with respect to ϕ obtained by this investigation, because the deformation characteristics of normally consolidated sand samples are in general closely related to their strength characteristics.

It may be seen in Fig. 19 that the tendency of volume expansion when σ_3' is lower than around 0.1 kgf/cm^2 is slightly larger than as expected from the smooth change of volume change with the change of σ_3' which are indicated by broken lines. This tendency may be attributed to the strain hardening caused before the start of shearing. It is very likely that this kind of strain hardening induced some amount of volume decrease due to shear deformation, which is larger for a looser sample. This kind of extra volume decrease can be induced under the anisotropic stress conditions during the stages of the setting of cap and membrane and the saturation of sample. When triaxial compression tests are performed at a pressure

NII-Electronic Library Service

The Japanese Geotechnical Society

of as low as 0.02～0.05 kgf/cm^2, the effects of this kind of strain hardening may still be preserved in the deformation properties of the sample in the beginning of triaxial compression, resulting in decreasing the tendency of volume decrease or increasing the tendency of volume expansion. Therefore, it seems that if the strain hardening described above were not caused before the start of triaxial compression, the volume change characteristics at σ_3' less than around 0.1 kgf/cm^2 would have been such ones as indicated by broken lines shown in Fig. 19. Further researches will be needed to answer this question after improving the testing method more.

Furthermore, it may be seen in Fig. 20 that the axial strain values are larger for smaller values of σ_3' when σ_3' is less than around 0.05 kgf/cm^2. This may correspond to the fact that the value of stress ratio σ_1'/σ_3' or ϕ obtained at the mid-height of sample are underestimated ones as the maximum values of σ_1'/σ_3' within a sample at an extremely low stress. Further researches will also be needed in this respect.

CONCLUSIONS

The angle of internal friction $\phi=\arcsin\{(\sigma_1'-\sigma_3')/(\sigma_1'+\sigma_3')\}_{max}$ of saturated Toyoura sand and its deformation characteristics at extremely low pressures were measured by the conventional drained triaxial compression tests while paying great cautions to stress measurements. On the basis of the limited number of tests reported in this paper, the following were found:

(1) To obtain accurate values of ϕ at extremely low pressures, the effects of both membrane forces and self-weight of sample should be properly accounted for in calculating stresses within a sample.

(2) The angle of internal friction of saturated Toyoura sand does not change so much with the change of the minor principal stress σ_3' when σ_3' is lower than around 0.5 kgf/cm^2 (50 kN/m^2), all other things being equal. In particular, the change of ϕ with the change of σ_3' was found to be very small at σ_3' lower than around 0.1 kgf/cm^2 (9.8 kN/m^2). In using the Mohr-Coulomb failure criterion for saturated Toyoura sand, it is not needed to introduce the apparent cohesion intercept, using reasonable values of ϕ which decreases slightly at a rather constant rate as σ_3' increases.

(3) The deformation characteristics at large strains of saturated Toyoura sand change only slightly with the change of σ_3' when σ_3' is lower than around 0.5 kgf/cm^2 (50 kN/m^2), especially when σ_3' is lower than around 0.1 kgf/cm^2 (10 kN/m^2). This phenomenon corresponds well to such a trend in ϕ as described above.

ACKNOWLEDGEMENTS

The major part of this investigation was performed as a part of the Doctor of Engineering thesis work of the first author at the Institute of Industrial Science, the University of Tokyo, with the cooperations provided by Mr. O. Tadokoro, undergraduate student of the University of Nihon. The authors gratefully acknowledge the helpful discussions of Dr. F. Molenkamp, Delft Soil Mechanics Laboratory, the Netherlands, which were very useful to increase the accuracy of our testing methods. The staff members of the central workshop of the Institute fabricated the major parts of the apparatuses with the cooperations provided by Messrs. T. Sato and S. Yamada, colleagues of the authors. Miss M. Torimitsu helped the authors with preparing the draft. The authors are indebted to their colleagues above. Financial support provided by the Ministry of Education is also greatly acknowledged.

REFERENCES

1) Berre, T. (1982): "Triaxial testing at the Norwegian Geotechnical Institute," Geotechnical Testing Journal, ASTM, Vol. 5, No. 1/2,

NII-Electronic Library Service

The Japanese Geotechnical Society

March/June, pp. 3-17.

2) Duncan, J. M. and Seed, H. B. (1967) : "Corrections for strength test data," Jour. SM Div., Proc. ASCE, Vol. 93, No. SM 5, pp. 121-137.

3) Fukushima, S. (1982) : "Experimental study on deformation and strength characteristics of sand by torsional shear tests," Doctor of Eng. Thesis, University of Tokyo (in Japanese).

4) Henkel, D. J. and Gilbert, G. C. (1952) : "The effect of rubber on the measured triaxial compression strength of clay samples," Géotechnique, Vol. 3, pp. 20-29.

5) Molenkamp, F. and Luger, H. J. (1981) : "Modelling and minimization of membrane penetration effects in tests on granular soils," Géotechnique, Vol. 31, No. 4, pp. 471-486.

6) Ponce, V. M. and Bell, J. M. (1971) : "Shear strength of sand at extremely low pressures," Jour. of SMF Div., Proc. of ASCE, Vol. 97, No. SM 4, April, pp. 625-638.

7) Stroud, M. A. (1971) : "The behaviour of sand at low stress levels in the simple-shear apparatus," A dessertation submitted for the degree of Ph. D. at Cambridge Univ.

8) Tatsuoka, F. (1981) : "A simple method for automatic measurement of volume change in laboratory tests," Soils and Foundations, Vol. 21, No. 3, pp. 104-105.

9) Tatsuoka, F., Molenkamp, F., Torii, T. and Hino, T. (1984) : "Behavior of lubrication layers of platens in element tests," Soils and Foundations, Vol. 24, No. 1, pp. 113-128.

NII-Electronic Library Service